Dominant role of winds near Sri Lanka in driving seasonal sea level variations along the west coast of India

Iyyappan Suresh, Jérôme Vialard, Takeshi Izumo, Matthieu Lengaigne, W. Han, Julian P. Mccreary, Pillathu Moolayil Muraleedharan

AGU PUBLICATIONS

Geophysical Research Letters

RESEARCH LETTER
10.1002/2016GL069976

Key Points:
- Winds near Sri Lanka drive 60% of Indian west coast seasonal sea level
- Bay of Bengal wind forcing contributes to only 20%
- Winds near Sri Lanka are also essential for driving Lakshadweep high/low

Supporting Information:
- Supporting Information S1

Correspondence to:
I. Suresh,
isuresh@nio.org

Citation:
Suresh, I., J. Vialard, T. Izumo, M. Lengaigne, W. Han, J. McCreary, and P. M. Muraleedharan (2016), Dominant role of winds near Sri Lanka in driving seasonal sea level variations along the west coast of India, *Geophys. Res. Lett.*, *43*, 7028–7035, doi:10.1002/2016GL069976.

Received 18 APR 2016
Accepted 13 JUN 2016
Accepted article online 15 JUN 2016
Published online 2 JUL 2016

Dominant role of winds near Sri Lanka in driving seasonal sea level variations along the west coast of India

I. Suresh[1], J. Vialard[2], T. Izumo[2,3], M. Lengaigne[2,3], W. Han[4], J. McCreary[5], and P. M. Muraleedharan[1]

[1]CSIR-National Institute of Oceanography, Goa, India, [2]LOCEAN-IPSL, Sorbonne Université (UPMC, Université Paris 06)-CNRS-IRD-MNHN, Paris, France, [3]Indo-French Cell for Water Sciences, IISc-NIO-IITM-IRD Joint International Laboratory, CSIR-NIO, Goa, India, [4]Department of Atmospheric and Oceanic Sciences, University of Colorado Boulder, Boulder, Colorado, USA, [5]IPRC/SOEST, University of Hawai'i at Mānoa, Honolulu, Hawaii, USA

Abstract The strong seasonal cycle of sea level along the west coast of India (WCI) has important consequences for ecosystem and fisheries, and the Lakshadweep high/low in the southeast Arabian Sea is important for fisheries and the Indian summer monsoon. Previous studies suggested that WCI sea level variability is primarily driven by remote wind forcing from the Bay of Bengal and equatorial Indian Ocean through coastal Kelvin wave propagation. Using a linear ocean model, we demonstrate that wind forcing in a relatively small region around the southern tip of India and east of Sri Lanka contribute to ~60% of this variability. Wind variations from the rest of the Bay and the equator only account respectively for ~20% and ~10%. Sea level signals forced by the "southern tip" winds extend westward into the eastern Arabian Sea through Rossby wave propagation, with more than 50% contribution in the Lakshadweep high/low region.

1. Introduction

The seasonally reversing monsoon winds, a unique aspect of the tropical Indian Ocean, force a strong seasonal variability as manifested both in sea level and surface circulation of the North Indian Ocean (NIO) [e.g., *Schott and McCreary*, 2001]. The sea level along the west coast of India (WCI), in particular, is dominated by the seasonal cycle. Figure 1a, which shows the standard deviation of the observed seasonal sea level, indicates that the WCI is one of the regions in NIO with the largest seasonal variability. This variability further extends westward through Rossby wave (RW) propagation into the southeastern Arabian Sea, including a region known as the Lakshadweep high/low (LH/LL) [*Shankar and Shetye*, 1997]. The seasonal sea level (and hence thermocline depth) variability along the WCI and in the LH/LL has strong societal impacts. First, the seasonal upwelling during boreal summer along the WCI and in the southeastern Arabian Sea brings nutrients to the surface layer, causes phytoplankton bloom, and thus influences the food chain with a direct impact on fisheries [*Madhupratap et al*., 2001]. The upwelled water from the open ocean subsurface Oxygen Minimum Zone also leads to the formation of the world ocean's largest natural hypoxic system along the WCI, with strong implications for regional ecosystem and fisheries [*Naqvi et al*., 2000, 2009]. Finally, the deep thermocline associated with LH favors development of high sea surface temperatures in the southeastern Arabian Sea before the summer monsoon, well known as "Arabian Sea mini warm pool," which influences the southwest monsoon onset date [*Vinayachandran et al*., 2007], and total rainfall [*Masson et al*., 2005], which affects the lives of more than one billion people in India. It is therefore important to understand the processes that control the eastern Arabian Sea (WCI and LH/LL) sea level and thermocline variability.

In the past three decades, numerous studies (see review in *Amol et al*. [2014]) have focused on describing and understanding the seasonal cycle of sea level and surface currents along the WCI, i.e., the seasonally reversing West India Coastal Current (WICC) [*Shetye et al*., 1990]. Earlier studies [e.g., *Yu et al*., 1991] proposed that WCI sea level variations are strongly influenced by the remote equatorial wind forcing, through propagation of Kelvin waves (KWs) along the equator and coastal KWs around the rim of Bay of Bengal (BoB). Using a 2.5-layer model, *McCreary et al*. [1993] demonstrated that the seasonal WCI sea level variations are primarily wind driven and are largely remotely forced by BoB winds, rather than the local winds with weak alongshore component as they blow normal to coast. *Shankar et al*. [2002] performed a series of sensitivity experiments with 1.5-layer model to isolate the effect of alongshore winds in WCI from those along the BoB western rim (including both the east coasts of India and Sri Lanka). They concluded that the BoB alongshore winds excite coastal KWs that propagate

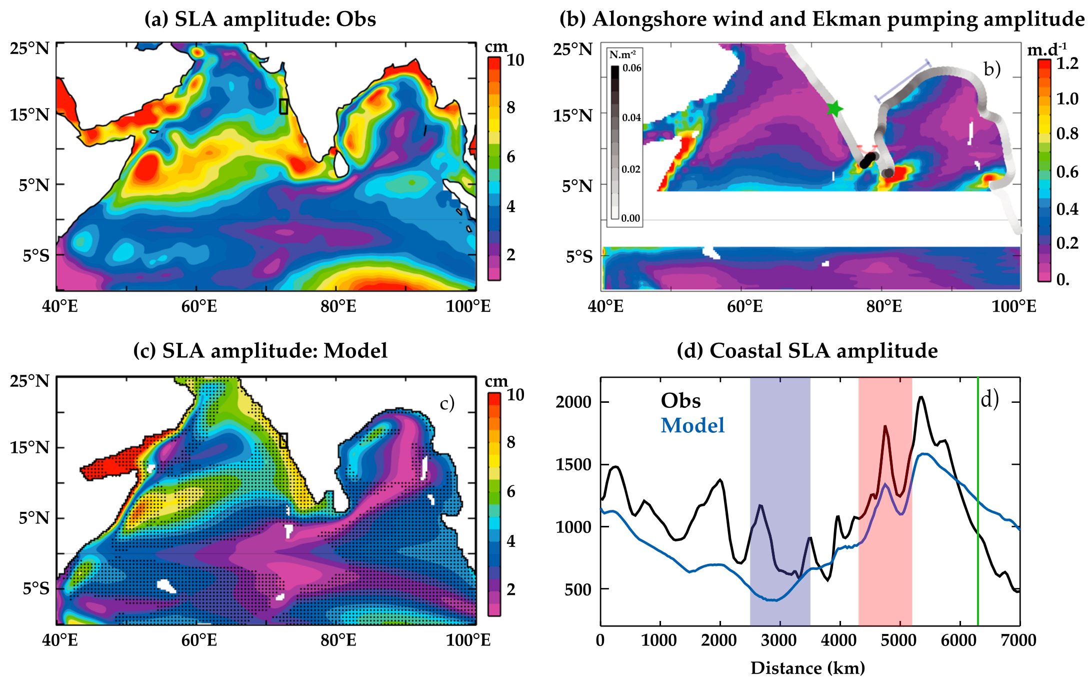

Figure 1. (a) Standard deviation of observed seasonal sea level. (b) Standard deviation of seasonal Ekman pumping velocity (m d^{-1}, color shaded) and alongshore wind stress (grey shades along the coastline; grey scale inset). (c) Same as Figure 1a but for modeled seasonal sea level. The regions where the correlation between the observed and modeled seasonal sea level is more than 0.8 are hatched. (d) Standard deviation of seasonal sea level normalized by the square root of the Coriolis parameter, averaged over a 50 km cross-shore extent, as a function of distance along the NIO coastal waveguide from the entrance of BoB waveguide at the eastern BoB rim. The above normalization eliminates the increasing wave amplitude associated with the narrowing coastal waveguide toward higher latitudes [e.g., *Gill*, 1982]. The blue (red) shaded vertical band in Figure 1d marks the region of strong alongshore forcing in the northwestern BoB (southern tip of India-Sri Lanka) identified by a marker of the same color in Figure 1b. The green vertical line in Figure 1d marks 15°N on the WCI, also marked with a green star in Figure 1b and black frames in Figures 1a and 1c.

southward along the east coast of India, bend around Sri Lanka, and further propagate northward along the WCI to influence the WICC. Those remotely forced sea level signals along the WCI radiate away as RWs, resulting in the formation of LH/LL [*Shankar and Shetye*, 1997] and impact regions as far as Somali coast in the western Arabian Sea [*McCreary et al.*, 1993; *Beal et al.*, 2013].

Figure 1b highlights the regions with strong, localized seasonal variations in the alongshore wind stress and Ekman pumping velocity. The northwestern BoB and the southern tip of India and Sri Lanka (hereafter "STIP" region; Figure S1 in the supporting information) exhibit strong alongshore wind stress forcing (Figure 1b) as the southwest and northeast monsoon winds blow parallel to the coast there. A strong Ekman pumping signal is also evident off the east coast of Sri Lanka (Figure 1b) [*Vinayachandran and Yamagata*, 1998]. The resulting sea level anomalies will propagate westward as RWs and induce signals at the Sri Lankan coast, which can in principle set up coastal KWs and impact the sea level and currents downstream along the WCI. Figure 1d shows the standard deviation of the observed sea level seasonal cycle in the NIO coastal waveguide. Though coastal sea level amplitude starts increasing in the region of strong alongshore forcing in the northwestern BoB, the increase is far larger in the STIP vicinity, strongly suggesting that the wind variations in this region are important for large-amplitude seasonal cycle downstream on the WCI. Thus, the alongshore wind stress and offshore Ekman transport variations in the STIP, which only represents less than 20% of the total area of BoB, could play a dominant role on WCI sea level variability, and potentially also in the LH/LL region.

Though BoB forcing in the earlier modeling studies [*McCreary et al.*, 1993; *Shankar et al.*, 2002] did include STIP wind variations, their importance for WCI seasonal cycle relative to the rest of BoB have so far not been discussed. Moreover, the above studies provided only a qualitative, rather than quantitative, assessment of the relative importance of BoB against WCI wind forcing. In the present study, we aim to quantify the relative roles of all major forcing regions (equator, BoB, and local forcing) on the seasonal sea level variations along the WCI and in the LH/LL. We demonstrate that despite its small size, the STIP region is the major contributor

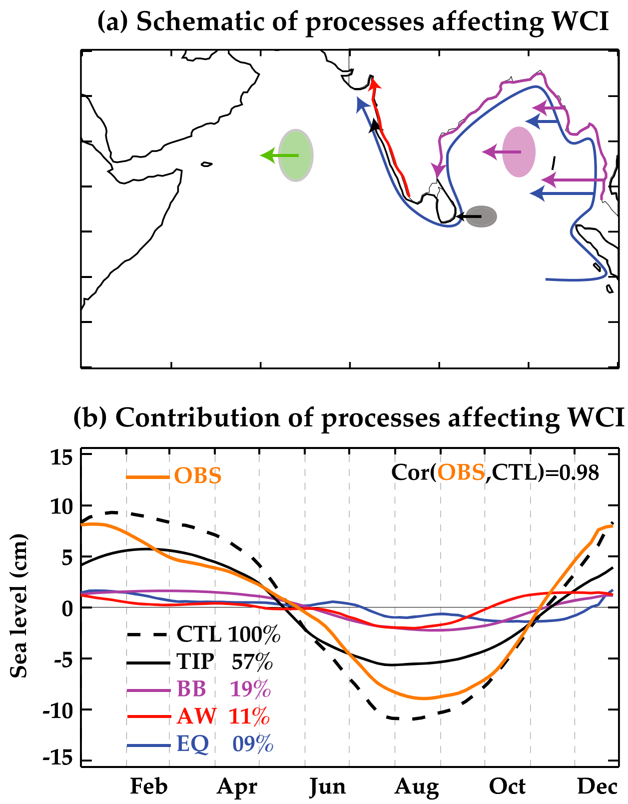

Figure 2. (a) Schematic representation of the processes that influence the sea level off the WCI (forcing from the southern tip of India (TIP; black), Bay of Bengal (BB; purple), west coast of India (AW; red), and equatorial EQ (blue) regions; see section 2.2 for details). (b) CTL experiment sea level seasonal cycle at 15°N on the WCI (black frame in Figure 1c; dashed black curve) and its decomposition into the processes above. Figures 2a and 2b use consistent color codes. The observed seasonal cycle is shown in orange. The percentage contributions of each process to the CTL sea level seasonal cycle are indicated in Figure 2b.

among the total BoB forcing. To that end, we will use a linear ocean model that captures the observed sea level seasonal cycle reasonably well. Details of our model and of the process solutions, which allow us to quantify contributions from various mechanisms, are provided in section 2. The results are presented in section 3, and section 4 summarizes our major findings with a discussion on the results.

2. The Model and Sensitivity Experiments

2.1. Model and Its Validation

We use a modified version of *McCreary et al.* [1996] linear, continuously stratified model [*Suresh et al.*, 2013], detailed in the supporting information (hereafter supporting information). The shallow water equations are solved individually for the first five vertical baroclinic modes, and the model solution is obtained as their sum (solutions obtained with 20 modes are very similar to the ones presented in this paper). The model equations are discretized over a 0.25° resolution grid for the Indian Ocean domain (30°S–30°N, 30°E–110°E), with a coastline derived from 200 m isobath. The model is forced with daily TropFlux wind stress [*Praveen et al.*, 2013] anomalies relative to the long-term mean over 1979–2013. The model solution described above is referred to as the control (CTL) experiment.

The sea level from CTL experiment is validated against the Archiving, Validation, and Interpretation of Satellite Oceanographic data altimeter observations (www.aviso.oceanobs.com/fr/accueil/index.html). Figures 1a and 1c suggest that our linear model correctly reproduces the observed amplitude and phase of the sea level seasonal cycle in most of the basin (hatched regions indicate where the correlation of CTL with the observed seasonal cycle is greater than 0.8), except in eddy-dominated regions (western BoB and western Arabian Sea), where nonlinear effects are important. The agreement is especially good all along the WCI (correlations exceeding 0.8 along the entire coast), our main region of interest (Figure 1c). For instance, the modeled sea level seasonal cycle on the WCI at 15°N is similar to the observed one, with a very similar amplitude and correlation coefficient of 0.98 (Figure 2b). Finally, our model also reproduces well the amplitude of the seasonal cycle all along the rim of the NIO (though with a slight underestimation, Figure 1d), particularly the increase in sea level amplitude in the vicinity of the STIP, indicating that it is well suited for our study.

2.2. Process Solutions

We group processes that can contribute to the sea level variability along the WCI and in the Arabian Sea as follows: contributions from (1) equatorial waveguide (EQ), (2) BoB forcing (BB), (3) winds over STIP region (TIP), (4) WCI alongshore winds (AW), and (5) interior Arabian Sea forcing (AS). Figure 2a provides a schematic of how each of these processes operates. Process EQ (dark blue in Figure 2a) includes all signals generated by the equatorial winds and transiting through the BoB coastal waveguide (part of this signal transits more slowly through the interior BoB as a result of RW radiation from the eastern BoB rim). Process BB (purple) includes the effects of alongshore forcing from the BoB (particularly, stronger over the northwestern BoB) and of interior BoB Ekman pumping. The response of STIP forcing is represented by TIP (black), which includes the effects of alongshore forcing and of seasonal Ekman pumping east of Sri Lanka. Process AW (red) accounts for WCI alongshore forcing. Finally, AS (light green) accounts for the response of interior Arabian Sea Ekman pumping. Although this process marginally contributes to the WCI sea level variability, it is considered here because it may influence the strong seasonality of LH/LL that will also be discussed in the later sections.

Following *McCreary et al*. [1996], we isolate each of the above processes using a set of sensitivity experiments. The effect of alongshore forcing is isolated using a special boundary condition, which filters out the local forcing of coastal KWs by allowing the Ekman flow to pass through the boundary. For example, AW is obtained as the difference between CTL and a process solution in which the above condition is applied along the entire WCI (indicated by red line in Figure 2a). A series of dampers are used in various regions to isolate specific processes. The EQ, for example, is isolated from an experiment where a damper is applied in the entire equatorial region between 4°S and 4°N, with a 1° ramp at the northern and southern edges to minimize spurious effects. The resulting solution is free from equatorial forcing, and the difference from CTL thus yields the effect of only the equatorial forcing. Other processes are obtained in a similar way using dedicated sensitivity experiments, which are described in Supporting Information. As will be discussed in section 4, the results of our study are not very sensitive to other reasonable choices of the dampers used for the process solutions.

The linearity of our model, the choice of dampers, and the special boundary conditions ensure that sea level from each of these process solutions add up to that from the CTL (see Supporting Information for details). In the following, we will quantify the pointwise contribution of each process to the CTL seasonal sea level over the entire year by estimating the regression coefficient of the sea level seasonal cycle in each process solution to that in CTL. By construction, those coefficients add up to 1 (100%) and can be negative if a process interferes destructively with others to contribute to the sea level along the WCI.

3. Results

Figure 3 displays the August sea level climatology from the CTL solution (and the associated wind stress forcing), along with contributions from each process mentioned in section 2.2 and in Figure 2a. The month of August has been selected because it is representative of the contribution of each process to the CTL sea level seasonal cycle over the entire year, which is shown as contours of regression coefficients (see section 2.2) in Figure 3. Figure 2b further shows the full seasonal cycle and its decomposition at 15°N on the WCI (other locations on WCI display very similar behavior).

Figure 2b indicates that ~57% of the seasonal sea level variability at 15°N on the WCI is driven by the STIP forcing, i.e., the alongshore forcing and Ekman pumping over STIP region (Figures 1b and 2a). Figure 3b further illustrates the dominance of STIP forcing, with more than 50% contribution all along the WCI. The Ekman pumping induced by the strong cyclonic (anticyclonic) wind stress curl east of Sri Lanka during summer (winter) results in upwelling (downwelling) RWs, which propagate westward and set up upwelling (downwelling) KWs along the southeast coast of Sri Lanka. This upwelling (downwelling) signal is further reinforced by the winds (Figures 3a and 3b), which blow parallel to the coast during summer (winter) monsoon. We further separated the effect of alongshore wind stresses from that associated with Ekman pumping east of Sri Lanka in an additional experiment (see Supporting Information) in which the special boundary condition described in section 2 is only applied in the STIP region (not shown). The ~60% contribution of TIP to the WCI sea level seasonal cycle is dominated by alongshore forcing (~40%), with Ekman pumping off the east coast of Sri Lanka contributing to the remaining ~20%. As these coastal KWs propagate poleward along the WCI, the TIP contribution decreases by about 10% from the southern to the northern ends of the WCI due to RW radiation (Figure 3b).

Though BoB forcing (BB) is the second largest contributor to the WCI sea level seasonal cycle, it is much weaker (~19%, Figures 2b and 3c) than the TIP contribution. This weaker BB contribution is due to a combination of factors. Because of the BoB geometry and the alignment of northeast and southwest monsoonal

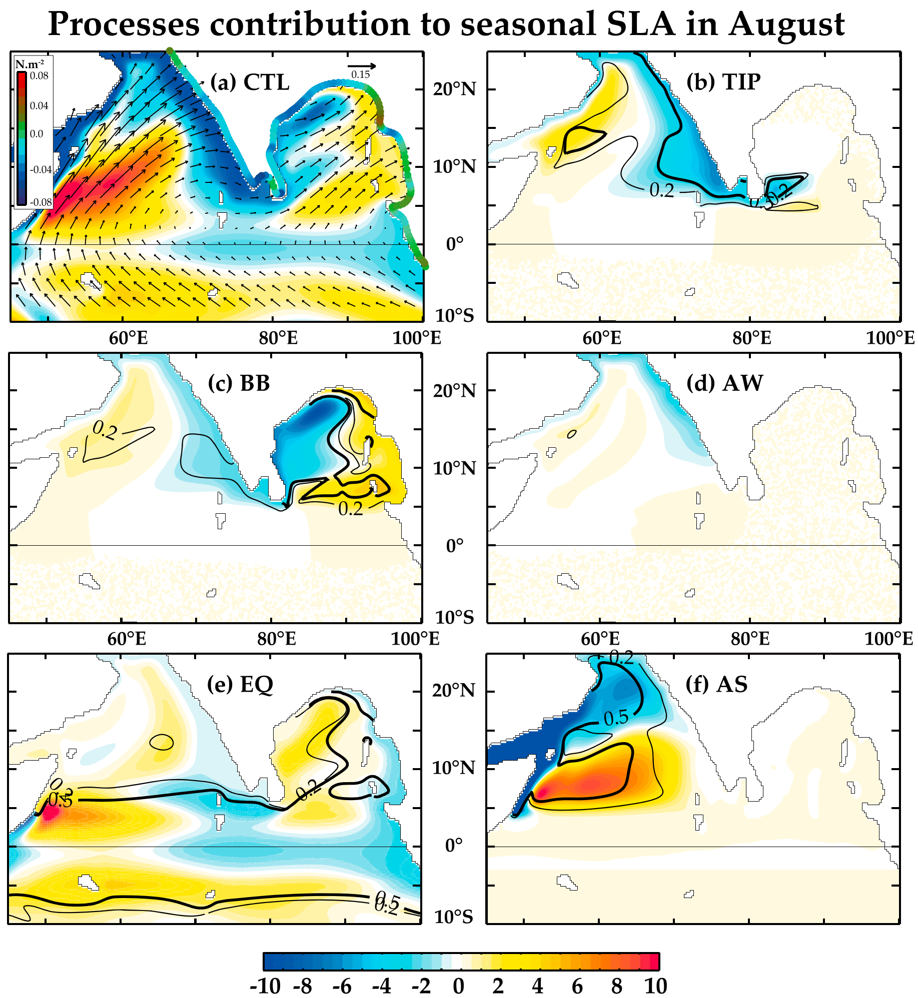

Figure 3. Climatological sea level (cm) and wind stress (N/m^2) for August from (a) the CTL experiment and its decomposition into the processes indicated in Figure 2a: (b) TIP, (c) BB, (d) AW, (e) EQ, and (f) AS. The alongshore wind stress (N/m^2) is indicated with a different color shading (see color bar inset) along the coastline in Figure 3a. Thick (thin) black line contours indicate contributions above 50% (20%) over the entire year, estimated from regression coefficients.

winds, the alongshore forcing tends to produce opposite polarity coastal signals in the eastern and western rims of the bay. As the propagation time (~1 week) of the coastal KW between the eastern and western BoB rims is short relative to the seasonal timescale, this results in a phase opposition and hence a weak coastal KW amplitude in the northwestern BoB. The local minimum in coastal sea level amplitude along the northwestern BoB (Figures 1a, 1c, and 3c) primarily results from the destructive interference of sea levels driven by the local upwelling-favorable winds (for the month of August) with those driven by the upstream downwelling-favorable winds. The wind stress curl in the southern Andaman Sea (Figure 1b) provides another source of destructive interference: this wind stress curl indeed forces RWs of opposite polarity to coastal KWs in the western BoB. During August, for example, a downwelling RW is induced in the southern BoB that interferes destructively with the upwelling signals propagating in the coastal waveguide east of Sri Lanka (Figure 3c).

The destructive interferences between eastern and western BoB signals resulting from both alongshore and interior forcing lead to an overall reduction of the amplitude of the coastal KW signals (along western and southwestern BoB) that bend around Sri Lanka to the WCI. Another probable cause for the weaker effect of BB than TIP is that the Ekman pumping east of Sri Lanka, due to its proximity to the equator, is much stronger than that in the rest of the BoB (Figure 1b). Finally, the dissipation may act more on the BB signals, which have a longer pathway along coastal waveguide to travel to the WCI. All of these factors collectively tend to produce a weaker contribution of BB than TIP to the WCI sea level seasonal cycle. As for the TIP process, offshore RW radiation also reduces the BB contribution as the coastal KWs propagate poleward along the WCI.

The WCI wind seasonal anomalies blow almost normal to the coast during both summer (Figure 3a) and winter (not shown) monsoons, resulting in a weak alongshore component. Consequently, the AW contribution is rather weak and accounts for only ~11% of the WCI seasonal sea level variations (Figures 3d and 2b). There is a marginal northward increase in the AW contribution that results from the integration of forcing downstream along the wave path. As was remarked by earlier studies [e.g., *McCreary et al*., 1993; *Shankar et al*., 2002], the phasing of the seasonal cycle driven by local forcing (red curve in Figure 2b) cannot explain the phasing of the total sea level seasonal cycle there (black dashed curve in Figure 2b). It is particularly clear in October when local winds favor downwelling, but the sea level is still negative (upwelling) relative to the annual mean (Figure 2b). This upwelling signal along WCI is largely driven by the TIP and BB processes, both being upwelling favorable at this time of the year and almost in phase over the entire seasonal cycle.

The reflection of equatorial KWs at the eastern boundary is associated with coastal KW propagation along the NIO coastal waveguide and RW radiation from the eastern BoB rim, and both can influence the sea level along the WCI. While EQ process dominates the seasonal cycle in the eastern BoB ($>$50%; Figure 3e), its contribution rapidly decreases toward the western BoB, ultimately resulting in only ~9% contribution along the WCI (Figure 2b). Two arguments can explain this very modest contribution of EQ along the WCI. First, the seasonal sea level at the entrance of the coastal waveguide (near Sumatra coast) is much weaker than the coastal signals generated by alongshore forcing in the BoB and STIP. Second, the sea level signals originating from the equator are further weakened at the east coast of India by the destructive interference between the coastal KWs and the RWs transiting through the interior BoB (not shown), leading to very weak coastal KW signals that propagate to the WCI.

We have so far been concerned with the sea level seasonal cycle along the WCI. The sea level signals along the WCI radiate westward as RWs, which combine with the signals induced by the interior Ekman pumping to influence the sea level in the interior Arabian Sea. The wind variations near Sri Lanka, being the dominant process in driving the seasonal sea level along the WCI, extend their strong influence westward into the interior Arabian Sea through RWs. Figure 3b indeed demonstrates the dominant role of STIP forcing (~60%) for the formation of the LH/LL. Farther west, the local Arabian Sea Ekman pumping dominates the sea level seasonal cycle, especially in the Somali upwelling region.

4. Discussion

Our model results demonstrate that the major source (~60%) of seasonal sea level variability along the WCI and in the eastern Arabian Sea is the wind variability in a relatively small region (less than 20% of the total BoB area) near the southern tip of India and Sri Lanka (with respective contributions of ~40% by winds along this convoluted coast and ~20% by Ekman pumping induced by the strong wind stress curl off the east coast of Sri Lanka). Our results further indicate that the contribution from the rest of BoB, which includes alongshore winds in BoB rim and interior BoB forcing, is less than 20% of the total WCI seasonal sea level cycle. This is partly due to the geometry of the BoB basin and the dominant wind forcing patterns, which result in the partial cancelation of signals forced in the eastern and western portions of the BoB. This refines findings from the previous literature [e.g., *McCreary et al*., 1993; *Shankar et al*., 2002]. Using a similar approach to ours, these studies concluded that the WICC and associated sea level changes along the WCI are primarily driven by the BoB alongshore winds but did not offer any quantification. The dominant role of wind forcing in the STIP region relative to the rest of the BoB was also not identified before.

The equatorial wind forcing, which was also emphasized by previous studies for the WICC, contributes less than 10% to the sea level along WCI. Consistent with earlier studies, the local alongshore winds are relatively less important for the seasonal cycle along WCI, with only ~10% contribution mainly during the summer monsoon. This weak contribution results from the monsoonal wind seasonal variations along WCI (north of 10°N) being nearly normal to the coast, with a weak alongshore component, driving a weak coastal KW response.

Seasonal sea level signals along the WCI radiate westward as RWs. As a corollary, our results also imply that the STIP wind forcing is an important contributor ($>$50%) to sea level seasonal cycle in the eastern Arabian Sea, especially in the LH/LL region (~60%). Farther west (west of 65°E), the strong Arabian Sea local forcing dominates.

We have tested the sensitivity of our results to the choice of wind forcing, dampers, and model parameters. Similar results are obtained by repeating the model experiments using QuikSCAT wind stresses (available from http://cersat.ifremer.fr/data/), which also shows dominance of STIP winds, contributing ~57% to the WCI seasonal sea level variability (Table S2 in Supporting Information). The dampers used here were designed to minimize the distortions in the model solutions, especially at the edges of the dampers by ramping the signals linearly to zero within 1° from the edges (see Supporting Information). This is ensured from the contribution maps (Figure 3), which show almost no spurious patterns. Repeating our experiments with a 2° ramp for dampers yields nearly identical contributions (Table S2), indicating that our results are not sensitive to the exact design of these dampers. Experiments with other dampers (e.g., a damper in the eastern Indian Ocean as in *McCreary et al.* [1996] to isolate EQ process) also give very similar results (not shown). Finally, the lateral friction used in our solution may also influence the results, since the coastal KWs have narrow offshore structure and propagate over long distances. Reducing our frictional coefficient by an order of magnitude results in contributions similar to those discussed in the paper (Table S2), with STIP being the major driver of the seasonal sea level variations along WCI. Our results are thus robust and insensitive to different observational wind products, the model parameters, and the choices of experimental setup, with TIP being the major contributor to the WCI seasonal cycle (57 to 69%), followed by a modest (19 to 23%) contribution of forcing from the rest of the BoB.

We have shown that STIP wind variations dominate the sea level (and hence thermocline) variability in a large portion of the eastern Arabian Sea. They play a key role in the WCI seasonal upwelling, which strongly impacts the regional ecosystem and fisheries [e.g., *Naqvi et al.*, 2009] and in the formation of the LH and "Arabian Sea mini warm pool" that influences the monsoon [e.g., *Vinayachandran et al.*, 2007]. This is not only an interesting academic example of scale interactions, where wind variations in a relatively small region have large-scale consequence, but also has practical implications. Our results may, for example, be a good incentive for a better monitoring of winds in this region or may imply that atmospheric resolution in coupled models does matter to realistically simulate the sea level in the eastern Arabian Sea.

Given the strong role of STIP wind forcing at the seasonal scale, one may wonder if it also matters at intraseasonal and interannual timescales [*Amol et al.*, 2012]. We know from *Suresh et al.* [2013] that the WCI intraseasonal sea level variations are mostly remotely forced from the equatorial region, suggesting a weak role of STIP winds at these timescales. Previous studies of NIO interannual sea level variability have mainly focused on the BoB. While interannual variability is weaker along the west than along the east coast of India [e.g., *Aparna et al.*, 2012], it may, however, have more important societal consequences. As noted in section 1, WCI hypoxia occurs during late boreal summer and fall when the remote wind forcing near the STIP favors upwelling (Figure 2b), bringing the subsurface hypoxic waters close to the surface. In those conditions, even a weak WCI interannual variability can act to either enhance or suppress hypoxic events [*Parvathi et al.*, 2016]. This emphasizes the need to better understand the WCI interannual sea level variability. Is the wind variability in STIP important for the WCI interannual sea level variability as demonstrated for the seasonal timescale or weak as expected for the intraseasonal timescale? What are the reasons explaining these different contributions at various timescales? We will investigate these questions in a later study.

Acknowledgments
I.S. thanks Director, CSIR-NIO, Pankajakshan and Neetu for their encouragement and acknowledges the funding from Indian National Centre for Ocean Information Services (HOOFS), Hyderabad, and Council of Scientific and Industrial Research, New Delhi. J.V., M.L., and T.I. acknowledge the funding from the CNES AltiKa project. W. Han is supported by NASA Ocean Vector Wind Science Team award NNX14AM68G. The authors thank Dennis Moore and an anonymous reviewer for their valuable comments. This is NIO contribution 5901.

References

Amol, P., D. Shankar, S. G. Aparna, S. S. C. Shenoi, V. Fernando, S. R. Shetye, A. Mukherjee, Y. Agarvadekar, S. Khalap, and N. P. Satelkar (2012), Observational evidence from direct current measurements for propagation of remotely forced waves on the shelf off the west coast of India, *J. Geophys. Res.*, *117*, C05017, doi:10.1029/2011JC007606.

Amol, P., et al. (2014), Observed intraseasonal and seasonal variability of the West India Coastal Current on the continental slope, *J. Earth Syst. Sci.*, *123*(5), 1045–1074, doi:10.1007/s12040-014-0449-5.

Aparna, S. G., J. P. McCreary, D. Shankar, and P. N. Vinayachandran (2012), Signatures of Indian Ocean Dipole and El Niño–Southern Oscillation events in sea level variations in the Bay of Bengal, *J. Geophys. Res.*, *117*, C10012, doi:10.1029/2012JC008055.

Beal, L. M., V. Hormann, R. Lumpkin, and G. R. Foltz (2013), The response of the surface circulation of the Arabian Sea to monsoonal forcing, *J. Phys. Oceanogr.*, *43*(9), 2008–2022, doi:10.1175/JPO-D-13-033.1.

Gill, A. E. (1982), *Atmosphere–Ocean Dynamics*, pp. 664, Academic Press, New York.

Madhupratap, M., T. C. Gopalakrishnan, P. Haridas, and K. K. C. Nair (2001), Mesozooplankton biomass, composition and distribution in the Arabian Sea during the Fall Intermonsoon: Implications of oxygen gradients, *Deep Sea Res., Part II*, *48*, 1345–1368.

Masson, S., et al. (2005), Impact of barrier layer on winter-spring variability of the southeastern Arabian Sea, *Geophys. Res. Lett.*, *32*, L07703, doi:10.1029/2004GL021980.

McCreary, J. P., Jr., P. K. Kundu, and R. L. Molinari (1993), A numerical investigation of dynamics, thermodynamics and mixed-layer processes in the Indian Ocean, *Prog. Oceanogr.*, *31*(3), 181–244, doi:10.1016/0079-6611(93)90002-U.

Mccreary, J. P., W. Han, D. Shankar, and S. R. Shetye (1996), Dynamics of the East India Coastal Current. 2. Numerical solutions, *J. Geophys. Res.*, *101*, 13,993–14,010, doi:10.1029/96JC00560.

Naqvi, S. W. A., D. A. Jayakumar, P. V. Narvekar, H. Naik, V. V. S. S. Sarma, W. D'Souza, S. Joseph, and M. D. George (2000), Increased marine production of N_2O due to intensifying anoxia on the Indian continental shelf, *Nature*, *408*, 346–349.

Naqvi, S. W. A., H. Naik, D. A. Jayakumar, A. K. Pratihary, G. Narvenkar, S. Kurian, R. Agnihotri, M. S. Shailaja, and P. V. Narvekar (2009), Seasonal anoxia over the western Indian continental shelf, in *Indian Ocean: Biogeochemical Processes and Ecological Variability*, edited by J. D. Wiggert et al., AGU, Washington, D. C., doi:10.1029/2008GM000745.

Parvathi, V., et al. (2016), Positive Indian Ocean Dipole events prevent anoxia along the west coast of India, *Biogeosci. Discuss.*, doi:10.5194/bg-2016-195.

Praveen, K. B., J. Vialard, M. Lengaigne, V. S. N. Murty, M. J. McPhaden, M. Cronin, F. Pinsard, and K. Gopala Reddy (2013), TropFlux wind stresses over the tropical oceans: Evaluation and comparison with other products, *Clim. Dyn.*, *40*, 2049–2071.

Schott, F. A., and J. P. McCreary (2001), The monsoon circulation of the Indian Ocean, *Prog. Oceanogr.*, *51*, 1–123.

Shankar, D., and S. R. Shetye (1997), On the dynamics of the Lakshadweep high and low in the southeastern Arabian Sea, *J. Geophys. Res.*, *102*(C6), 12,551–12,562, doi:10.1029/97JC00465.

Shankar, D., P. N. Vinayachandran, and A. S. Unnikrishnan (2002), The monsoon currents in the North Indian Ocean, *Prog. Oceanogr.*, *52*(1), 63–120, doi:10.1016/S0079-6611(02)00024-1.

Shetye, S. R., A. D. Gouveia, S. S. C. Shenoi, D. Sundar, G. S. Michael, A. M. Almeida, and K. Santanam (1990), Hydrography and circulation off the west coast of India during the southwest monsoon 1987, *J. Mar. Res.*, *48*, 359–378.

Suresh, I., J. Vialard, M. Lengaigne, W. Han, J. McCreary, F. Durand, and P. M. Muraleedharan (2013), Origins of wind-driven intraseasonal sea level variations in the North Indian Ocean coastal waveguide, *Geophys. Res. Lett.*, *40*, 5740–5744, doi:10.1002/2013GL058312.

Vinayachandran, P. N., and T. Yamagata (1998), Monsoon response of the sea around Sri Lanka: Generation of thermal domes and anticyclonic vortices, *J. Phys. Oceanogr.*, *28*(10), 1946–1960.

Vinayachandran, P. N., D. Shankar, J. Kurian, F. Durand, and S. S. C. Shenoi (2007), Arabian Sea mini warm pool and the monsoon onset vortex, *Curr. Sci.*, *93*(2), 203–214.

Yu, L., J. J. O. Brien, and J. Yang (1991), On the remote forcing of the circulation in the Bay of Bengal, *J. Geophys. Res.*, *96*(C11), 20,449–20,454, doi:10.1029/91JC02424.